Published in final edited form as:
Dev Biol. 2012 November 1; 371(1): 47–56. doi:10.1016/j.ydbio.2012.08.003.

Ectodermal-derived Endothelin1 is required for patterning the distal and intermediate domains of the mouse mandibular arch

Andre L.P. Tavares, **Elvin L. Garcia**[‡], **Katherine Kuhn**, **Crystal M. Woods**, **Trevor Williams**, and **David E. Clouthier**[§]
Department of Craniofacial Biology, University of Colorado Anschutz Medical Campus, Aurora, CO 80045, USA

Abstract

Morphogenesis of the vertebrate head relies on proper dorsal-ventral (D-V) patterning of neural crest cells (NCC) within the pharyngeal arches. Endothelin-1 (Edn1)-induced signaling through the endothelin-A receptor (Ednra) is crucial for cranial NCC patterning within the mandibular portion of the first pharyngeal arch, from which the lower jaw arises. Deletion of Edn1, Ednra or endothelin-converting enzyme in mice causes perinatal lethality due to severe craniofacial birth defects. These include homeotic transformation of mandibular arch-derived structures into more maxillary-like structures, indicating a loss of NCC identity. All cranial NCCs express *Ednra* whereas *Edn1* expression is limited to the overlying ectoderm, core paraxial mesoderm and pharyngeal pouch endoderm of the mandibular arch as well as more caudal arches. To define the developmental significance of Edn1 from each of these layers, we used Cre/*lox*P technology to inactivate *Edn1* in a tissue-specific manner. We show that deletion of *Edn1* in either the mesoderm or endoderm alone does not result in cellular or molecular changes in craniofacial development. However, ectodermal deletion of *Edn1* results in craniofacial defects with concomitant changes in the expression of early mandibular arch patterning genes. Importantly, our results also both define for the first time in mice an intermediate mandibular arch domain similar to the one defined in zebrafish and show that this region is most sensitive to loss of Edn1. Together, our results illustrate an integral role for ectoderm-derived Edn1 in early arch morphogenesis, particularly in the intermediate domain.

Keywords

neural crest cell; conditional knockout; mouse; endothelin; craniofacial

INTRODUCTION

Cranial neural crest cells (NCCs), a multipotent cell population generated at the interface between the non-neural ectoderm and neural tube, form most of the craniofacial structures, including bone, cartilage, connective tissue and portions of the cranial nerves (Bronner-Fraser, 1995; Le Douarin et al., 1993). During development of the upper and lower jaws,

[§]Correspondence address: David E. Clouthier. Ph.D., Department of Craniofacial Biology, University of Colorado Anschutz Medical Campus, Aurora, CO 80045, USA, Phone: 011-303-724-4565, FAX: 011-303-724-4580, david.clouthier@ucdenver.edu.
[‡]Present address: Department of Atmospheric Science, Colorado State University, Fort Collins, CO 80523, USA

NCCs migrate ventrally around the embryo and populate the pharyngeal arches, initiating a mesenchymal differentiation program (Le Douarin, 1982; Lumsden et al., 1991). Dorsal-ventral (D-V) patterning of this preskeletal NCC-derived mesenchyme is dependent on signals generally arising from the surrounding cell types within the arches (Chai and Maxson, 2006; Clouthier et al., 2010). Many of these signals act in both instructive and inhibitory manners that enforce sub-domains within the pharyngeal arches necessary for the development of regionally restricted bone, cartilage and connective tissue structures.

One of the key initiators of D-V patterning within the first mandibular arch NCCs is endothelin-1 (Edn1) (Clouthier et al., 2010), which is expressed by cells in the pharyngeal arch environment, including the ventral arch ectoderm, core paraxial mesoderm and pharyngeal arch endoderm (Clouthier et al., 1998; Maemura et al., 1996; Yanagisawa et al., 1998a; Yanagisawa et al., 1998b), while its cognate receptor, the endothelin-A receptor (*Ednra*) is expressed by NCCs that populate the pharyngeal arches (Clouthier et al., 1998; Yanagisawa et al., 1998a). Disruption of Ednra signaling leads to loss of NCC polarity and thus an expansion of the dorsal (proximal in mouse) identity into the ventral (distal in mouse) arch. This includes homeotic transformation of lower jaw structures and middle ear structures into more maxillary-like structures (Kimmel et al., 2003; Nair et al., 2007; Ozeki et al., 2004; Ruest et al., 2004; Sato et al., 2008) and inappropriate ventral expression of *jag1b* and *hey1* (the latter induced by Jagged-Notch signaling (Zuniga et al., 2010)).

Since *Edn1* is expressed in multiple domains in the developing arches, a fundamental question remains concerning the contribution of each domain to patterning. Studies in zebrafish have supported a role for *Edn1* expressed in the ectoderm, but the relevance of these findings to the mammalian system has been confounded by the presence of two copies of Ednra in the zebrafish as well as by differences in the morphogenesis of the lower jaw between fish and mammals. In particular, Edn1 is most important for the intermediate domain in the fish, which will form the joint between Meckel's cartilage and the palatoquadrate, whereas this latter structure is not present in mammals. Although an intermediate domain has not previously been noted in mammals, pharmacological antagonism of Ednra signaling resulted in disproportionate changes in gene expression within the central mandibular arch (Clouthier et al., 2003). In this study, we have taken advantage of Cre/*lox*P technology to disrupt *Edn1* expression in the first arch ectoderm, endoderm or mesoderm. We find that changes in facial patterning only occur when *Edn1* is inactivated in the ectoderm. In addition, this approach has unexpectedly allowed us to define the intermediate domain of the mandibular arch in mice and identify its structural significance. Our findings point to this domain as a crucial signaling center in mammalian lower jaw development.

MATERIALS AND METHODS

Mice

The generation, characterization and genotyping protocols for $Edn1^{flox/flox}$ ($Edn1^{fl/fl}$) (Kisanuki et al., 2010), *Foxg1-Cre* (Hebert & McConnell, 2000), *Myf5-Cre* (Tallquist *et al.*, 2000; Jackson Laboratories strain B6.129S4-$Myf5^{tm3(cre)Sor}$/J), $Foxa2^{mcm}$ (Park *et al.*, 2008) and *R26R* (Soriano, 1999) mice have been previously described. The Crect transgene is comprised of an ectodermal enhancer of *Tfap2a* driving *Cre* expression in the ectoderm (Forni *et al., 2011*).

Generation of mutant embryos

To generate conditional knockout embryos, $Edn1^{fl/+}$;*Cre* mice were bred with $Edn1^{fl/fl}$ mice to generate $Edn1^{fl/fl}$;*Foxg1-Cre*, $Edn1^{fl/fl}$;*Myf5-Cre*, $Edn1^{fl/fl}$;$Foxa2^{mcm}$ and $Edn1^{fl/fl}$;*Crect*

embryos. Because the *Foxa2-Cre* construct is tamoxifen-inducible, embryonic day (E) 6.5 pregnant female mice received tamoxifen. To accomplish this, tamoxifen was first dissolved in 100% ethanol at 10 mg/100 μl. Mineral oil was added to obtain a final concentration of 10 mg/ml. After sonicating for 45 min, progesterone was added at 5 mg/ml (which can limit fetal toxicity of tamoxifen (Jackson Laboratories)) and then the tamoxifen/progesterone mixture used immediately. Pregnant mice were weighed and then injected intraperitoneally with 75 μg per gram body weight of the tamoxifen/progesterone mixture.

Confirmation of allele recombination

Cre-mediated recombination analysis of the $Edn1^{flox}$ allele was performed as described (Kisanuki et al., 2001) using DNA extracted with the Puregene Tissue Core Kit A (Gentra) from E9.0 wild type and mutant embryo pharyngeal arches. Briefly, extracted DNA was measured using a Nanodrop ND-1000 spectrophotometer (Nanodrop) and 20 ng/μl of genomic DNA was added to each PCR reaction. The reactions, performed with the same settings previously described (Kisanuki et al., 2001), generate a 300 bp product for the recombined allele.

β-galactosidase staining

Whole-mount staining was performed as previously described (Ruest et al., 2003). Briefly, embryos were collected between embryonic day (E) 8.0 to E10.5, fixed in 4% paraformaldehyde (PFA) on ice for 1 hour then processed for β-galactosidase staining overnight at room temperature. After staining, embryos were rinsed and photographed on an Olympus SZX12 stereomicroscope fitted with a DP11 digital camera. For more detailed analysis of staining, these stained E9.0 embryos were embedded in Paraplast Plus tissue embedding medium and sectioned at 12 μm. Sections were collected on Pluscoated slides (Fisher) and counterstained with nuclear fast red as previously described (Ruest et al., 2003). Sections were analyzed and photographed using an Olympus BX51 compound microscope fitted with a DP71 digital camera.

Skeleton staining

Cartilage staining of E13.5 and E14.5 embryos with alcian blue was performed as previously described (Clouthier et al., 1998). Skeletal staining of E18.5 embryos with alizarin red (bone) and alcian blue (cartilage) was performed as previously described (Ruest et al., 2004). Stained embryos were analyzed and photographed using the Olympus SZX12 stereomicroscope as described above.

Whole-mount in situ hybridization

Whole-mount single probe in situ hybridization (ISH) analysis was performed as described previously (Clouthier *et al.*, 1998) using digoxigenin (DIG)-labeled antisense cRNA riboprobes against *Dlx2, Dlx3, Dlx5, Hand2* and *Goosecoid*. For dual probe whole-mount in situ hybridization, fluorescein-labeled antisense cRNA riboprobes against *Dlx3* and *Dlx5* were used in combination with DIG-labeled riboprobes against *Bapx1/Nkx3.2*. Processing and hybridization was identical to that of the single probe protocol, though maleic acid buffer plus Tween-20 (MABT) was used for embryo washes. Embryos were blocked with MABT + 2% blocking reagent (Roche) + 20% sheep serum, incubated overnight with 1:2,000 anti-fluorescein-AP antibody (Roche) in blocking solution, washed with MABT and developed with magenta-phos (Biosynth) in pH 8.5 NTMT. The first AP enzyme was killed by incubating developed embryos in 65°C MABT for 1 hour. After this step, embryos were blocked again, incubated with 1:2,000 anti-digoxigenin-AP antibody (Roche) in blocking solution and developed with BCIP (Roche) in pH 9.5 NTMT. Embryos were photographed using an Olympus SZX12 microscope as described above.

RESULTS

Early expression domains of *Foxg1-Cre, Myf5-Cre, Foxa2^{mcm} and Crect*

To inactivate *Edn1* in a tissue-specific manner, we used four Cre transgenic mouse strains: *Foxg1-Cre* (endoderm/mesoderm/ectoderm) (Hebert & McConnell, 2000), *Crect* (ectoderm) (Forni *et al., 2011*), *Myf5-Cre* (mesoderm)(Tallquist *et al.*, 2000) and *Foxa2^{mcm}* (endoderm) (Park et al., 2008). To first confirm that Cre-mediated *lox*P recombination occurred in a spatio-temporal manner sufficient to delete *Edn1* prior to or during Edn1 function (which is between E8.5 and E9.0 (Ruest and Clouthier, 2009)). Cre animals were crossed into the *R26R* strain (Soriano, 1999). Embryos were harvested between E8.0 (6 somites) and E10.5 (35 somites) and stained for beta-galactosidase (β-gal) activity. In *Foxg1-Cre* embryos, Cre sequence has been inserted into the *Foxg1* locus (Hebert & McConnell, 2000). In *R26R;Foxg1-Cre* embryos, β-gal activity was observed by 6 somites (E8.0) in the endoderm/foregut region and the first arch (Fig. 1A). At 10 and 20 somites (E8.5 and E9.0, respectively), foregut staining was still present, with staining also present in the pharyngeal arches and frontonasal prominence (Fig. 1B, C). Transverse sections through these stained embryos illustrated that β-gal staining was confined to the arch ectoderm (arrowheads), pharyngeal pouch endoderm, and core paraxial mesodermal cells (Fig. 1E). Staining at 25 somites (E9.5; Fig. 1D) appeared similar to that observed at 20 somites. Based on this staining, the *Foxg1-Cre* strain would likely result in an almost complete inactivation of *Edn1* within the arches, providing a good control when examining the phenotypes resulting from the use of our other more tissue-specific Cre strains.

We next analyzed β-gal staining in *R26R;Crect* embryos. This strain expresses *Cre* under the regulation of a *Tfap2* α ectodermal-specific enhancer (T. Williams, manuscript in preparation). Cre activity was detected in the first pharyngeal arch ectoderm (arrow in Fig. 1F, G) and frontonasal prominence by 10 somites (E8.5; Fig. 1F), with the staining intensity increasing by 20 somites (E9.0; Fig. 1H). β-gal staining was also present in the otic vesicle, trigeminal ganglion and optic placode between 15 and 20 somites (Fig. 1G–I). β-gal staining extended to the ectoderm of more caudal pharyngeal arches by 20 somites (E9.0; Fig. 1H). Transverse sections of these embryos showed that most arch ectodermal cells were β-gal-positive (Fig. 1J). This pattern remained unchanged at 35 somites (E10.5) (Fig. 1I).

In the *Myf5-Cre* strain, a *Cre* cDNA has been inserted into the *Myf5* locus so that *Cre* expression is under control of *Myf5* regulatory sequences (Tallquist et al., 2000). β-gal staining in *R26R;Myf5-Cre* embryos was observed starting at 8 somites (E8.0) in the somatic mesoderm (Fig. 1K). At 12 somites (E8.5), we detected β-gal staining adjacent to the pharyngeal arches (Fig. 1L). By 20 somites (E9.0), this staining was restricted to the core mesoderm in the pharyngeal arches (Fig. 1M). Transverse sections through the arch of this embryo illustrated this restriction to the core mesoderm, though staining was faint (Fig. 1O and inset in Fig. 1O). By 25 somites (E9.5), the core mesoderm staining in the pharyngeal arches was robust (Fig. 1N).

Foxa2^{mcm} animals express a tamoxifen-inducible *Cre* cassette from the Forkhead box A2 (*Foxa2*) locus in the early embryos endoderm (Park et al., 2008). Following injection of pregnant *R26R;Foxa2^{mcm}* females with tamoxifen at a stage equivalent to E6.5, embryos were collected between 8 and 25 somites (E8.0 to E9.5). At 8 somites (E8.0), β-gal staining was observed in the foregut endoderm (Fig. 1P). By 10 somites, this staining was more intense (Fig. 1Q–S). β-gal staining was also detected in the first pharyngeal pouch endoderm (Fig. 1Q). By 20 somites (E9.0), this endodermal pouch staining was very intense (Fig. 1R). Transverse sections through the pharyngeal arch illustrated that expression was confined to the arch endoderm (Fig. 1T). Expression was unchanged at 25 somites (E9.5; Fig. 1R, S).

Cre expression drives recombination of the conditional *Edn1* locus

To first confirm that our *Cre* strains could delete our conditional *Edn1* allele, we crossed mice containing a conditional allele of the *Edn1* gene ($Edn1^{fl/fl}$) with the different *Cre* strains described above. Mandibular arches were collected from E9.0 embryos, with genomic DNA extracted and used in a recombination-specific PCR using primers that only detected the recombined *Edn1* allele (Kisanuki et al., 2001). While Ednra signaling is required as early as E8.5, maximum sensitivity to loss of Ednra signaling occurs at E9.0 (Ruest and Clouthier, 2009). In our recombination assay, primers flanking the deleted region of the allele were used for PCR; recombination of the floxed allele resulted in the presence of a 300 bp band. This band was observed in all $Edn1^{fl/fl}$;*Cre* embryos, indicating that the *Edn1* conditional allele was recombined by all four *Cre* strains (Fig. 2). This recombination band was robust for all samples except that from the mandibular arch of $Edn1^{fl/fl}$;$Foxa2^{mcm}$ embryos. Since robust recombination was observed in *R26R*;$Foxa2^{mcm}$ embryos (Fig. 1R, T) and each reaction contained an identical amount of input DNA, the low intensity of the recombined band in the $Edn1^{fl/fl}$;$Foxa2^{mcm}$ sample likely reflects the amount of endoderm that existed in the excised mandibular arch.

Ectodermal loss of *Edn1* leads to changes in craniofacial bone and cartilage development

To determine how tissue-specific loss of *Edn1* affected D-V patterning, we began our analysis of *Edn1* conditional mutants by examining E13.5 or 14.5 conditional knockout embryos for changes in cartilage development, since this is one of the earliest structural changes observed in endothelin-family knockouts in mice and fish (Clouthier et al., 1998; Miller et al., 2000). Deletion of *Edn1* in the pharyngeal arch ectoderm, pharyngeal pouch endoderm and core paraxial mesoderm of E14.5 $Edn1^{fl/fl}$;*Foxg1-Cre* embryos resulted in hypoplasia of Meckel's cartilage (Fig. 3B). There was also a gap in Meckel's cartilage at its proximal end where it failed to articulate with the malleus (Fig. 3B). In addition, the hyoid bone appeared more rostral in the pharynx of $Edn1^{fl/fl}$;*Foxg1-Cre* embryos (Fig. 3B), a finding observed in *Ednra, Edn1* and *Ece1* mutant embryos (Clouthier et al., 1998; Kurihara et al., 1994; Yanagisawa et al., 1998b). However, the overall phenotype was less severe than observed in $Edn1^{-/-}$ mutants (Kurihara et al., 1994). When *Edn1* was only deleted in the pharyngeal arch ectoderm of E14.5 $Edn1^{fl/fl}$;*Crect* embryos, Meckel's cartilage appeared slightly shortened, though its articulation with the malleus was normal (Fig. 3C). The hyoid bone positioning again appeared more rostral, but not to the same extent as observed in $Edn1^{fl/fl}$;*Foxg1-Cre* embryos (Fig. 3B). In contrast, Meckel's cartilage was unaffected in E14.5 $Edn1^{fl/fl}$;*Myf5-Cre* embryos (Fig. 3D). While we also attempted to examine changes in cartilage structures in E14.5 $Edn1^{fl/fl}$;$Foxa2^{mcm}$ embryos, administration of tamoxifen at E6.5 (shown to achieve optimal gene recombination at E8.5 (Park et al., 2008) resulted in embryo lethality by E14.5, a general problem with tamoxifen administration before E8.5 (Hayashi and McMahon, 2002). However, we were able to collect E13.5 $Edn1^{fl/fl}$;$Foxa2^{mcm}$ embryos; in these embryos, the development of Meckel's cartilage appeared normal in comparison to control embryos (Fig. 3E, F).

To further examine how tissue-specific *Edn1* loss affected skull development, we examined bone development in conditional knockout embryos. In E18.5 $Edn1^{fl/fl}$;*Foxg1-Cre* embryos, the lower jaw was shortened and contained mystacial vibrissae on the ectoderm (Fig. 4F and Supp. Fig. 1E). The presence of mystacial vibrissae on the ectoderm is observed in *Ednra, Edn1, Dlx5/Dlx6* and *Hand2* mutants (Barron et al., 2011; Depew et al., 2002; Ozeki et al., 2004; Ruest et al., 2004). Skeleton preparations of these embryos showed that the mandible was hypoplastic and malformed (Fig. 4G, J), though still retained a mandibular shape, suggesting that patterning of the distal arch mesenchyme was at least partially correct. This is contrast to $Edn1^{-/-}$ embryos, in which the mandible undergoes a homeotic transformation into a maxilla-like structure (Ozeki et al., 2004). However, duplicated palatine (p*) and jugal

(j*) bones were present in the lower jaw (Fig. 4G, J), suggesting that D-V patterning of NCC-derived mesenchyme was at least partially disrupted. In addition, tympanic ring bones were absent (yellow asterisks in Fig. 4G–I), the masseter muscle was dysmorphic (Supp. Fig. 1F) and an ectopic bone extended from the gonial bones to the pterygoid bones (Fig. 4I). This ectopic bone, while not present in *Edn1*$^{-/-}$ embryos (Ozeki et al., 2004), is observed in both *Ednra*$^{fl/fl}$*;Wnt1-Cre* embryos (Abe et al., 2007) and *Ednra*$^{-/-}$ < − > +/+ chimeric embryos (Clouthier et al., 2003) as well as in embryos from mothers treated for varying times with an Ednra antagonist (Ruest and Clouthier, 2009).

In E18.5 *Edn1*$^{fl/fl}$*;Crect* embryos, the retrognathia observed (Fig. 4K) was similar to that observed in *Edn1*$^{fl/fl}$*;Foxg1-Cre* embryos (Fig. 4F), and mystacial vibrissae were also present in both conditional knockout embryos (Supp. Fig. 1H). However, bone and cartilage staining of *Edn1*$^{fl/fl}$*;Crect* embryos revealed that the mandible bone was less dysmorphoic (Fig. 4L, M, O) than that of *Edn1*$^{fl/fl}$*;Foxg1-Cre* embryos (Fig. 4G, H, I). Appearing only slightly shorter, the primary finding was the presence of duplicated jugal bones (j* - Fig. 4L, O). All other mandibular first arch-derived bones were normal (Fig. 4L–O), though a cleft secondary palate was observed in some mutant embryos (Supp. Fig. 1H, I). In addition, the aberrant bone observed *Edn1*$^{fl/fl}$*;Foxg1-Cre* embryos (Fig. 4H, I) was not observed in *Edn1*$^{fl/fl}$*;Crect* embryos (Fig. 4N). In contrast, E18.5 *Edn1*$^{fl/fl}$*;Myf5-Cre* (Fig. 4P–T) embryos did not have any gross or skeletal changes in the lower jaw. In addition, these homozygous mutant mice were viable and fertile (data not shown). As described above, embryonic lethality at E14.5 of all embryos following tamoxifen administration prevented skeletal analysis of *Edn1*$^{fl/fl}$*;Foxa2*^{mcm} embryos.

Disruption of *Edn1* in the ectoderm causes *g*ene expression changes

To determine the molecular basis of these observed skeletal changes, we examined the expression of specific genes previously identified as being either induced or repressed downstream of Ednra signaling and crucial for D-V patterning of the mandibular arch. In E10.5 control embryos, *Dlx2* expression was observed in the proximal mandibular arch mesenchyme and along the ectoderm overlying the distal mandibular arch (Fig 5A). In E10.5 *Edn1*$^{fl/fl}$*;Foxg1-Cre* embryos, *Dlx2* expression was disrupted along most of the distal ectoderm of the mandibular arch (Fig. 5F) similar to that seen in *Ednra* mutants (Ruest et al., 2004). Unlike in *Ednra* mutant embryos, mesenchymal expression was not upregulated distally (Fig. 5F). *Dlx3* expression was completely lost in the mandibular arch mesenchyme and overlying ectoderm and reduced in the second arch (Fig. 5G and data not shown), again matching the pattern observed in *Ednra* mutant embryos (Ruest et al., 2004). *Dlx5* expression was also disrupted, but only in a band spanning the central mandibular arch (compare Fig. 5C, 5H). *Hand2* expression appeared unchanged (Fig. 5I), as did the expression of *Goosecoid* (Fig. 5J), a gene whose arch expression requires Hand2 (Barron et al., 2011); (Kimmel et al., 2003). Matching the milder phenotype, only *Dlx5* expression was disrupted in E10.5 *Edn1*$^{fl/fl}$*;Crect* embryos (Fig. 5M). However, as observed for *Edn1*$^{fl/fl}$*;Foxg1-Cre* embryos, this disruption was only observed in a band spanning the central mandibular arch. Expression of these markers was not disrupted in E10.5 in *Edn1*$^{fl/fl}$*;Myf5-Cre* (Fig. 5P–T) or *Edn1*$^{fl/fl}$*;Foxa2*^{mcm} (Fig. 5U–Y) embryos.

While the changes in the expression of both *Dlx3* and *Dlx5* were profound in *Edn1*$^{fl/fl}$*;Foxg1-Cre* embryos, these changes could result from either failure to initiate expression or failure to maintain expression. To determine which of these was occurring, we examined the expression of both genes in E9.5 *Edn1*$^{fl/fl}$*;Foxg1-Cre* embryos. When compared to control embryos (Fig 6A), *Dlx3* expression in mutants was almost completely absent, suggesting that its expression was never induced (Fig. 6B). While *Dlx5* expression was present, expression was confined to the distal half of the mandibular arch (Fig. 6D, F). Expression was absent in the proximal half of the arch, suggesting that the observed

expression of *Dlx5* in this region in E10.5 *Edn1$^{fl/fl}$;Foxg1-Cre* embryos is induced by a different signaling pathway.

Disruption of *Dlx5* gene expression demarcates the intermediate domain in the mouse mandibular arch

Our in situ hybridization results illustrate that *Dlx5* expression in both E10.5 *Edn1$^{fl/fl}$;Foxg1-Cre* and *Edn1$^{fl/fl}$;Crect* embryos is only affected in a narrow band in the central arch (Fig 5H, M, Fig. 7B, F and Fig. 8B, F). Since this area corresponds spatially to the intermediate domain of the zebrafish mandibular arch, we performed additional analysis to define the gene expression pattern within this region, first examining gene expression changes in *Edn1$^{fl/fl}$;Foxg1-Cre* embryos. *Nkx3.2* (*Bapx1*) is the primary molecular marker of the intermediate domain in zebrafish (Miller et al., 2003; Talbot et al., 2010) and a key molecule required for zebrafish jaw joint development (Miller et al., 2003). In E10.5 control embryos, *Nkx3.2* expression was confined to a caudal region in the central mandibular arch mesenchyme in addition to a small region along the rostral arch ectoderm (Fig. 7C). In E10.5 *Edn1$^{fl/fl}$;Foxg1-Cre* embryos, expression in the caudal mesenchyme was downregulated, though arch ectoderm expression was unaffected. To confirm that the *Nkx3.2* expression domain correlated with the domain in which *Dlx5* expression was lost, we performed double in situ hybridization analysis. In E10.5 control embryos, *Nkx3.2* mesenchyme expression was contained within the *Dlx5* expression domain (Fig. 7E). In E10.5 *Edn1$^{fl/fl}$;Foxg1-Cre* embryos, the remaining ectodermal *Nkx3*.2 expression domain was centered in the domain in which *Dlx5* was absent (Fig. 7F), strongly suggesting that this *Dlx5*-free domain is the *Nkx3.2* positive intermediate domain.

Like *Nkx3.2, Dlx3* is also a marker of the intermediate domain of zebrafish (Talbot et al., 2010). As described above, *Dlx3* expression in control embryos is expressed in the proximo-caudal mesenchyme of the mandibular arch and the distal arch ectoderm (Fig. 5B and Fig. 7G), though the region was larger than that of *Nkx3.2* (Fig. 7C). In *Edn1$^{fl/fl}$;Foxg1*-Cre embryos, the *Dlx3* mesenchyme expression was almost completely absent (Fig. 5G and Fig. 7H). To verify that *Nkx3.2* and *Dlx3* expression domains overlapped in the mouse arch, we again preformed double in situ hybridization analysis. In E10.5 control embryos, *Nkx3.2* mesenchyme expression (blue) was indeed contained within the *Dlx3* mesenchyme domain (magenta) (Fig. 7I), though the normal mandibular arch expression domain of *Dlx3* was difficult to observe due to the overlying *Nkx3*.2 expression (compare Fig. 7C, G, I). In *Edn1$^{fl/fl}$;Foxg1-Cre* embryos, the *Dlx5* expression-free domain corresponded to the region in which *Nkx3*.2 mesenchyme expression was absent and the expression of *Dlx3* was severely downregulated (Fig. 7J).

This data suggests that an intermediate domain does exist in the mouse mandibular arch and that Edn1/Ednra signaling is required to establish and/or maintain gene expression in this domain. To prove that this function is due to ectoderm-derived Edn1, we repeated our in situ analysis in E10.5 *Edn1$^{fl/fl}$;Crect* embryos. As described above, *Dlx5* expression in *Edn1$^{fl/fl}$;Crect* embryos was disrupted in a band across the middle portion of the arch (Fig. 8B). This region corresponded to the *Nkx3.2* mesenchymal expression domain in control embryos (Fig. 8C) and the region in which *Nkx3.2* expression was lost in *Edn1$^{fl/fl}$;Crect* embryos (Fig. 8D). This finding was confirmed in *Edn1$^{fl/fl}$;Crect* embryos following double in situ hybridization analysis of *Nkx3.2/Dlx5* expression, in which expression of *Dlx5* and *Nkx3.2* were both lost in the same central arch domain. These findings support the idea that the ectoderm is the source of Edn1 critical for establishing/defining the intermediate domain of the mandibular arch.

DISCUSSION

Edn1 is a crucial signaling factor that establishes the D-V patterning of the pharyngeal arches. Here we have demonstrated using conditional gene inactivation that the ectoderm appears to be the required source of Edn1 during mandibular arch patterning and that this requirement appears most important in the intermediate arch domain.

Ectoderm is a required source of Edn1 during patterning of the mandibular first pharyngeal arch

Using Cre/*lox*P technology, we have taken advantage of mouse genetics to illustrate that the cranial ectoderm is a critical source of Edn1 during facial morphogenesis in mammals. All *Cre* strains used in this work were able to recombine the *R26R* allele by E8.5/E9.0, the time period during which Ednra signaling is required for D-V patterning of the mouse pharyngeal arches (Ruest and Clouthier, 2009). We also showed that the conditional *Edn1* allele is recombined by E9.0 using all four *Cre* strains. While not quantitative, the recombination band observed in $Edn1^{fl/fl};Foxa2^{mcm}$ embryos was by far the weakest. While it is possible that this *Cre* strain produces a poor recombination efficiency of floxed alleles, we note that $Foxa2^{mcm}$-mediated recombination of the *R26R* allele appears robust (Fig. 1P–T and (Park et al., 2008)). More likely, the limited recombination seen using PCR reflects the amount of endoderm contained within the mandibular arch sample used for our assay. Further, because the preproendothelin-1 mRNA has a short intracellular half-life of around 15 minutes (Inoue et al., 1989), we do not believe that mRNA present before gene recombination could significantly contribute to Ednra signaling after Cremediated recombination.

In both $Edn1^{fl/fl};Foxg1\text{-}Cre$ and $Edn1^{fl/fl};Crect$ embryos, defects in lower jaw structures were present including the presence of duplicated maxillary structures. This was accompanied by a partial loss of *Dlx5* and *Nkx3.2* in both strains and a loss of *Dlx3* in $Edn1^{fl/fl};Foxg1\text{-}Cre$ embryos. Together, our results illustrate that Edn1 from the ectoderm is likely the most crucial source of Edn1 during D-V patterning of the pharyngeal arches. However, a complete loss of mandibular identity as seen in *Edn1, Ednra* or *Dlx5/Dlx6* knockout mice (Beverdam et al., 2002; Depew et al., 2002; Ozeki et al., 2004; Ruest et al., 2004) was not observed even when *Edn1* was inactivated in the ectoderm, endoderm and core mesoderm using the *Foxg1-Cre* strain. One explanation for this partial phenotype is the timing of recombination. The jaw phenotype and related gene expression changes observed in $Edn1^{fl/fl};Foxg1\text{-}Cre$ embryos resemble that of embryos following Ednra antagonism between E8.5 and E9.0 (Ruest and Clouthier, 2009). In this case, normal D-V patterning of the arches would be initiated but then lost, with differential effects observed in the distal and intermediate domains (see below). Another possibility is that the *Foxg1-Cre* strain did not elicit complete *Edn1* inactivation throughout the entire tissue. If conditional gene inactivation was incomplete spatially and/or temporally, residual Edn1 could limit the extent of a jaw phenotype. We also cannot rule out the possibility that endoderm-specific loss of Edn1 could later lead to changes in bone development within the head, as while $Edn1^{fl/fl};Foxa2^{mcm}$ embryos did not show changes in gene expression, we could not generate E18.5 embryos for analysis of bone and cartilage structures. Likewise, we cannot rule out the possibility that Edn1 from all three arch tissues (ectoderm, mesoderm and endoderm) works in concert to pattern the arches. This could explain the less severe phenotype of $Edn1^{fl/fl};Crect$ embryos. However, together with the lack of gene expression changes observed in $Edn1^{fl/fl};Myf5\text{-}Cre$ and $Edn1^{fl/fl};Foxa2^{mcm}$ embryos and the short half live of *Edn1* mRNA (Inoue et al., 1989), our data suggest that, as in zebrafish (Miller et al., 2000; Miller et al., 2003; Nair et al., 2007), the Edn1 produced by these layers is not crucial for patterning of the first mandibular arch. This argument is strengthened by recent findings illustrating that while the endoderm is required to achieve normal size and shape of jaw

cartilages, it is not required for earlier D-V patterning of the NCC-derived mesenchyme (Balczerski et al., 2012).

Identification of the mouse intermediate domain of the mandibular pharyngeal arch

The most intriguing change observed when *Edn1* was inactivated in the ectoderm was loss of *Dlx5* expression in a rostrocaudal stripe across the middle of the mandibular arch. We further showed that this domain can be defined by the expression of both *Dlx3* and *Nkx3.2*, downstream mediators of Ednra signaling. This location and expression profile matches the intermediate domain in zebrafish, which plays a crucial role in establishing the zebrafish jaw joint. Loss of zebrafish Edn1 leads to downregulation of *nkx3.2* and subsequent fusion of Meckel's cartilage and the palatoquadrate (Miller et al., 2003). In contrast, loss of Hand2 in both mouse and zebrafish embryos leads to expansion of the *Nkx3.2*/*nkx3.2* domain (Miller et al., 2003) and Tavares and Clouthier, unpublished). While *Nkx3.2* and *Dlx3* are expressed in the central mandibular arch of the mouse, it has been difficult to truly demarcate this domain and understand its functional significance. Here we have shown that the gene expression domains of both *Nkx3.2* and *Dlx3* in the mandibular arch corresponds to the central arch domain in which *Dlx5* expression is lost, thus marking this affected region as at least a portion of the mammalian intermediate arch domain. Fate mapping of this domain in zebrafish has shown that it gives rise to the dorsal aspects of ventral cartilages and the ventral aspects of dorsal cartilages (Talbot et al., 2010), hence its roll in joint development.

There are obvious differences between the jaw joints of fish and mammals. In zebrafish, Nkx3.2 is required for the proper formation of the jaw joint between Meckel's cartilage and the palatoquadrate (Miller et al., 2003). In the mouse, this joint appears to correlate with the articulation between the malleus and the incus (Tucker et al., 2004). While this articulation is not disrupted in mouse $Nkx3.2^{-/-}$ embryos, potentially due to evolutionary changes in *Gdf5/Gdf6* expression, two genes involved in joint formation, other middle ear structures are abnormal or missing (Tucker et al., 2004). This suggests that *Nkx3.2* (and by extension, *Dlx3*) do indeed mark the intermediate domain of the mammalian mandibular arch. Interestingly, the one common change in the skulls of $Edn1^{fl/fl}$;*Foxg1-Cre* and $Edn1^{fl/fl}$;*Crect* embryos is a duplication of the jugal bone that occurs concomitant with the loss of malleus and incus, a finding observed in endothelin mouse mutants (Ozeki et al., 2004; Ruest et al., 2004). In control embryos, the malleus and incus articulate through a fibrous joint. Likewise, in mutant embryos, the duplicated jugal bone articulates with the actual jugal bone of the zygomatic arch through a fibrous joint. Thus, while a change in identity of the intermediate domain NCCs has occurred in endothelin mutant embryos, the functional outcome (a joint) is unchanged. This suggests that patterning cues in the arch may occur or be confined by a functional registry that has not been fully appreciated.

The identity of the signals that drives jugal formation in the maxillary prominence is unknown. That a jugal bone forms in the mandibular arch mesenchyme of endothelin mutants could result from the action of mandibular arch signals that normally work with Ednra signaling to drive a different developmental fate. Alternatively, loss of Ednra signaling could result in the inappropriate upregulation of maxillary signals normally involved in jugal determination. The expression of multiple genes is upregulated in mandibular arch in the absence of Ednra signaling, including *Dlx2* (Ruest et al., 2004). Interestingly, targeted deletion of *Dlx2* leads to disruption of jugal formation (Qiu et al., 1997; Qiu et al., 1995). While we did not observe any gross changes in *Dlx2* expression, it is possible that mild changes in the *Dlx2* expression boundary sufficient to change the local fate of the mandibular mesenchyme could exist. Further molecular dissection of this region will be required to address these questions.

Sensitivity of the intermediate domain to loss of Ednra signaling

One question that remains from this and previous studies examining variable loss of Ednra signaling in mouse and zebrafish is why this intermediate domain is so sensitive to the level of Edn1. Our gene expression analysis of *Edn1*$^{fl/fl}$;*Foxg1-Cre* embryos illustrates that while distal expression of *Dlx5* is present at E9.5, normal proximal/intermediate expression is absent. However, by E10.5, the proximal expression of *Dlx5* has recovered while the intermediate expression is still absent. In addition, we have previously shown that following short-term pharmacological antagonism of Ednra signaling in mouse embryos, gene expression in this domain is the first and longest affected (Ruest and Clouthier, 2009). Taken together, the most likely explanations is that Edn1 initiates patterning in both the distal and intermediate domains, but recombination via the *Cre* strains we have used occurs after Edn1/Ednra signaling has initiated patterning cascades in the distal arch. In this case, we would expect that if *Edn1* were inactivated earlier in arch morphogenesis (E8.0–E8.25), we would more closely recapitulate the *Edn1/Ednra/Ece1* mutant phenotype (reviewed in (Clouthier et al., 2010). Further, our findings suggest that alternative mechanisms can compensate for loss of Ednra signaling to induce *Dlx5* expression in the proximal arch. Together, these findings illustrate that the uniform *Dlx5* expression pattern that exists in the mandibular arch of wild type embryos masks a far more complex and overlapping set of control mechanisms. Future advances in Cre transgenic mouse strains that activate earlier or target specific arch sub-domains should make these hypotheses testable.

The hypothesis presented above requires the action of one or more additional factors to maintain Edn1-induced signaling pathways within the distal mandibular arch following loss of Edn1. Our results clearly show that such a molecule would have to be distal-specific, since intermediate gene expression is neither initiated nor maintained. One candidate for this molecule could be a Bmp, as Bmp signaling in zebrafish appears to pattern the distal arch by inducing *edn1* expression and later maintaining Edn1-induced expression of *hand2* (Alexander et al., 2011). In addition, overexpression of *Bmp4* in mice leads to upregulation of *Hand2* expression independent of Dlx5/Dlx6 (Bonilla-Claudio et al., 2012). However, if a BMP-dependent pathway is involved in the mouse model, then Bmp2 and/or Bmp7 would be the most likely candidates, as ectodermal *Bmp4* expression is lost in *Ednra*$^{-/-}$ mutants (Ruest et al., 2004). Another factor that works in concert with Ednra signaling to induce *Dlx5/Dlx6* expression during mandibular arch development is Mef2c (Arnold et al., 2007; Miller et al., 2007). However, *mef2ca* mutant zebrafish embryos have jaw joint defects, suggesting that its function is not restricted to the distal/ventral arch (Miller et al., 2007). Closer examination of other distal/ventral ectodermal signals and their relationship with Ednra signaling may shed additional light on this question.

While less likely, another possibility is that the increased sensitivity of the intermediate domain to loss of Ednra signaling is due to differential competence of NCC populations within the arch to respond to Edn1. Whether this actually occurs is not clear, as Ednra signaling in the mouse is required in a cell autonomous manner in both distal and intermediate domain derivatives (Clouthier et al., 2003). However, extrapolation of findings from NCC fate mapping in the chick suggest that the mouse mandible (a distal arch derivative (Ruest et al., 2003)) is composed almost solely of posterior midbrain-derived NCCs, while more proximal structures, including the tympanic ring and gonial bones, also contain NCCs from rhombomeres 1 and 2 (Kontges and Lumsden, 1996). It is plausible that while midbrain versus r1/r2 NCC populations could be equally dependent on Ednra signaling, r1/r2 cells would be less competent to respond to the signal that rescues gene expression in the distal (midbrain-derived) arch in endothelin mutants. It is also possible that both populations are equally competent to respond to additional signals, but mechanisms exist to limit expression of the compensating factor to the distal domain. Detailed analysis of

Ednra signaling in these specific NCC populations will be required to answer these questions.

Supplementary Material

Refer to Web version on PubMed Central for supplementary material.

Acknowledgments

We would like to thank Alicia Navetta for technical assistance and James F. Martin and Anne M. Moon for the tamoxifen-inducible *Foxa2*^{mcm} mice. This work was supported by NIH/NIDCR research grant DE014181 (to D.E.C.). The NIH had no involvement in the design, data collection and interpretation or the decision to submit this article for publication.

References

Abe M, Ruest L-B, Clouthier DE. Fate of cranial neural crest cells during craniofacial development in endothelin-A receptor deficient mice. Int. J. Dev. Biol. 2007; 51:97–105. [PubMed: 17294360]

Alexander C, Zuniga E, Blitz IL, Wada N, LePabic P, Javidan Y, Zhang T, Cho KW, Crump JG, Schilling TF. Combinatorial roles for Bmps and Endothelin 1 in patterning the dorsal-ventral axis of the craniofacial skeleton. Development. 2011; 138:5135–5146. [PubMed: 22031543]

Arnold MA, Kim Y, Czubryt MP, Phan D, McAnally J, Qi X, Shelton JM, Richardson JA, Bassel-Duby R, Olson EN. MEF2C transcription factor controls chondrocyte hypertrophy and bone development. Dev. Cell. 2007; 12:377–389. [PubMed: 17336904]

Balczerski B, Matstani M, Castillo P, Osborne N, Stainier DY, Crump JG. Analysis of sphingosine-1-phosphate signaling mutants reveals endodermal requirements for the growth but not the dorsoventral patterning of jaw skeletal precursors. Dev. Biol. 2012; 362:230–241. [PubMed: 22185793]

Barron F, Woods C, Kuhn K, Bishop J, Howard MJ, Clouthier DE. Downregulation of *Dlx5* and *Dlx6* expression by Hand2 is essential for initiation of tongue morphogenesis. Development. 2011; 138:2249–2259. [PubMed: 21558373]

Beverdam A, Merlo GR, Paleari L, Mantero S, Genova F, Barbieri O, Janvier P, Levi G. Jaw transformation with gain of symmetry after *Dlx5/Dlx 6* inactivation: mirror of the past. Genesis. 2002; 34:221–227. [PubMed: 12434331]

Bonilla-Claudio M, Wang J, Bai Y, Klysik E, Selever J, Martin JF. Bmp signaling regulates a dose-dependent transcriptional program to control facial skeletal development. Development. 2012; 139:709–719. [PubMed: 22219353]

Bronner-Fraser M. Origins and developmental potential of the neural crest. Exp. Cell Res. 1995; 218:405–417. [PubMed: 7796877]

Chai Y, Maxson J, R E. Recent advances in craniofacial morphogenesis. Dev. Dyn. 2006; 235:2353–2375. [PubMed: 16680722]

Clouthier DE, Garcia E, Schilling TF. Regulation of facial morphogenesis by endothelin signaling: insights from mouse and fish. Am. J. Med. Genet. A. 2010; 152A:2962–2973. [PubMed: 20684004]

Clouthier DE, Hosoda K, Richardson JA, Williams SC, Yanagisawa H, Kuwaki T, Kumada M, Hammer RE, Yanagisawa M. Cranial and cardiac neural crest defects in endothelin-A receptor-deficient mice. Development. 1998; 125:813–824. [PubMed: 9449664]

Clouthier DE, Williams SC, Hammer RE, Richardson JA, Yanagisawa M. Cell-autonomous and nonautonomous actions of endothelin-A receptor signaling in craniofacial and cardiovascular development. Dev. Biol. 2003; 261:506–519. [PubMed: 14499656]

Depew MJ, Lufkin T, Rubenstein JL. Specification of jaw subdivisions by *Dlx* genes. Science. 2002; 298:381–385. [PubMed: 12193642]

Hayashi S, McMahon AP. Efficient recombination in diverse tissues by a tamoxifen-inducible form of Cre: A tool for temporally regulated gene activation/Inactivation in the mouse. Dev. Biol. 2002; 244:305–318. [PubMed: 11944939]

Inoue A, Yanagisawa M, Takuwa Y, Mitsui Y, Kobayashi M, Masaki T. The human preproendothelin-1 gene. J. Biol. Chem. 1989; 264:14954–14959. [PubMed: 2670930]

Kimmel CB, Ullmann B, Walker M, Miller CT, Crump JG. Endothelin 1-mediated regulation of pharyngeal bone development in zebrafish. Development. 2003; 130:1339–1351. [PubMed: 12588850]

Kisanuki YY, Hammer RE, Miyazaki J, Williams SC, Richardson JA, Yanagisawa M. Tie2-Cre transgenic mice: a new model for endothelial cell-lineage analysis *in vivo*. Dev. Biol. 2001; 230:230–242. [PubMed: 11161575]

Kontges G, Lumsden A. Rhombencephalic neural crest segmentation is preserved throughout craniofacial ontogeny. Development. 1996; 122:3229–3242. [PubMed: 8898235]

Kurihara Y, Kurihara H, Suzuki H, Kodama T, Maemura K, Nagai R, Oda H, Kuwaki T, Cao W-H, Kamada N, Jishage K, Ouchi Y, Azuma S, Toyoda Y, Ishikawa T, Kumada M, Yazaki Y. Elevated blood pressure and craniofacial abnormalities in mice deficient in endothelin-1. Nature. 1994; 368:703–710. [PubMed: 8152482]

Le Douarin, NM. The neural crest. New York: Cambridge Univ Press; 1982.

Le Douarin NM, Ziller C, Couly GF. Patterning of neural crest derivatives in the avian embryo: in vivo and in vitro studies. Dev. Biol. 1993; 159:24–49. [PubMed: 8365563]

Lumsden A, Sprawson N, Graham A. Segmental origin and migration of neural crest cells in the hindbrain region of the chick embryo. Development. 1991; 113:1281–1291. [PubMed: 1811942]

Maemura K, Kurihara H, Kurihara Y, Oda H, Ishikawa T, Copeland NG, Gilbert DJ, Jenkins NA, Yazaki Y. Sequence analysis, chromosomal location, and developmental expression of the mouse preproendothelin-1 gene. Genomics. 1996; 31:177–184. [PubMed: 8824799]

Miller CT, Schilling TF, Lee K-H, Parker J, Kimmel CB. *sucker* encodes a zebrafish Endothelin-1 required for ventral pharyngeal arch development. Development. 2000; 127:3815–3838. [PubMed: 10934026]

Miller CT, Swartz ME, Khuu PA, Walker MB, Eberhart JK, Kimmel CB. *mef2ca* is required in cranial neural crest to effect Endothelin1 signaling in zebrafish. Dev. Biol. 2007; 308:144–157. [PubMed: 17574232]

Miller CT, Yelon D, Stainier DY, Kimmel CB. Two *endothelin 1* effectors, *hand2* and *bapx1*, pattern ventral pharyngeal cartilage and the jaw joint. Development. 2003; 130:1353–1365. [PubMed: 12588851]

Nair S, Li W, Cornell R, Schilling TF. Requirements for endothelin type-A receptors and endothelin-1 signaling in the facial ectoderm for the patterning of skeletogenic neural crest cells in zebrafish. Development. 2007; 134:335–345. [PubMed: 17166927]

Ozeki H, Kurihara Y, Tonami K, Watatani S, Kurihara H. Endothelin-1 regulates the dorsoventral branchial arch patterning in mice. Mech. Dev. 2004; 121:387–395. [PubMed: 15110048]

Park EJ, Sun X, Nichol P, Saijoh Y, Martin JF, Moon AM. System for tamoxifen-inducible expression of cre-recombinase from the *Foxa2* locus in mice. Dev. Dyn. 2008; 237:447–453. [PubMed: 18161057]

Qiu M, Bulfone A, Ghattas I, Meneses JJ, Christensen L, Sharpe PT, Presley R, Pedersen RA, Rubenstein JLR. Role of the Dlx homeobox genes in proximodistal patterning of the branchial arches: Mutations of Dlx-1, Dlx-2, and Dlx-1 and -2 alter morphogenesis of proximal skeletal and soft tissue structures derived from the first and second arches. Dev. Biol. 1997; 185:165–184. [PubMed: 9187081]

Qiu M, Bulfone A, Martinez S, Meneses JJ, Shimamura K, Pedersen RA, Rubenstein JLR. Null mutation of *Dlx-2* results in abnormal morphogenesis of proximal first and second branchial arch derivatives and abnormal differentiation in the forebrain. Genes Dev. 1995; 9:2523–2538. [PubMed: 7590232]

Ruest L-B, Dager M, Yanagisawa H, Charité J, Hammer RE, Olson EN, Yanagisawa M, Clouthier DE. *dHAND-Cre* transgenic mice reveal specific potential functions of dHAND during craniofacial development. Dev. Biol. 2003; 257:263–277. [PubMed: 12729557]

Ruest LB, Clouthier DE. Elucidating timing and function of endothelin-A receptor signaling during craniofacial development using neural crest cell-specific gene deletion and receptor antagonism. Dev. Biol. 2009; 328:94–108. [PubMed: 19185569]

Ruest LB, Xiang X, Lim KC, Levi G, Clouthier DE. Endothelin-A receptor-dependent and -independent signaling pathways in establishing mandibular identity. Development. 2004; 131:4413–4423. [PubMed: 15306564]

Sato T, Kurihara Y, Asai R, Kawamura Y, Tonami K, Uchijima Y, Heude E, Ekker M, Levi G, Kurihara H. An endothelin-1 switch specifies maxillomandibular identity. Proc. Natl. Acad. Sci. U S A. 2008; 105:18806–18811. [PubMed: 19017795]

Soriano P. Generalized *lacZ* expression with the ROSA26 Cre reporter strain. Nat. Gen. 1999; 21:70–71.

Talbot JC, Johnson SL, Kimmel CB. *hand2* and Dlx genes specify dorsal, intermediate and ventral domains within zebrafish pharyngeal arches. Development. 2010; 137:2507–2517. [PubMed: 20573696]

Tallquist MD, Weismann KE, Hellstrom M, Soriano P. Early myotome specification regulates PDFGA expression and axial skeleton development. Development. 2000; 127:5059–5070. [PubMed: 11060232]

Tucker AS, Watson RP, Lettice LA, Yamada G, Hill RE. Bapx1 regulates patterning in the middle ear: altered regulatory role in the transition from the proximal jaw during vertebrate evolution. Development. 2004; 131:1235–1245. [PubMed: 14973294]

Yanagisawa H, Hammer RE, Richardson JA, Williams SC, Clouthier DE, Yanagisawa M. Role of Endothelin-1/Endothelin-A receptor-mediated signaling pathway in the aortic arch patterning in mice. J. Clin. Invest. 1998a; 102:22–33. [PubMed: 9649553]

Yanagisawa H, Yanagisawa M, Kapur RP, Richardson JA, Williams SC, Clouthier DE, de Wit D, Emoto N, Hammer RE. Dual genetic pathways of endothelin-mediated intercellular signaling revealed by targeted disruption of endothelin converting enzyme-1 gene. Development. 1998b; 125:825–836. [PubMed: 9449665]

Zuniga E, Stellabotte F, Crump JG. Jagged-Notch signaling ensures dorsal skeletal identity in the vertebrate face. Development. 2010; 137:1843–1852. [PubMed: 20431122]

HIGHLIGHTS

- The source of endothelin-1 (Edn1) during pharyngeal arch morphogenesis is examined.
- Only loss of Edn1 from the ectoderm leads to defects in facial development.
- Conditional gene deletion of Edn1 allowed visualization of the intermediate domain.
- Intermediate arch gene expression was most sensitive to loss of Edn1.
- Loss of intermediate arch gene expression correlated with proximal jaw defects.

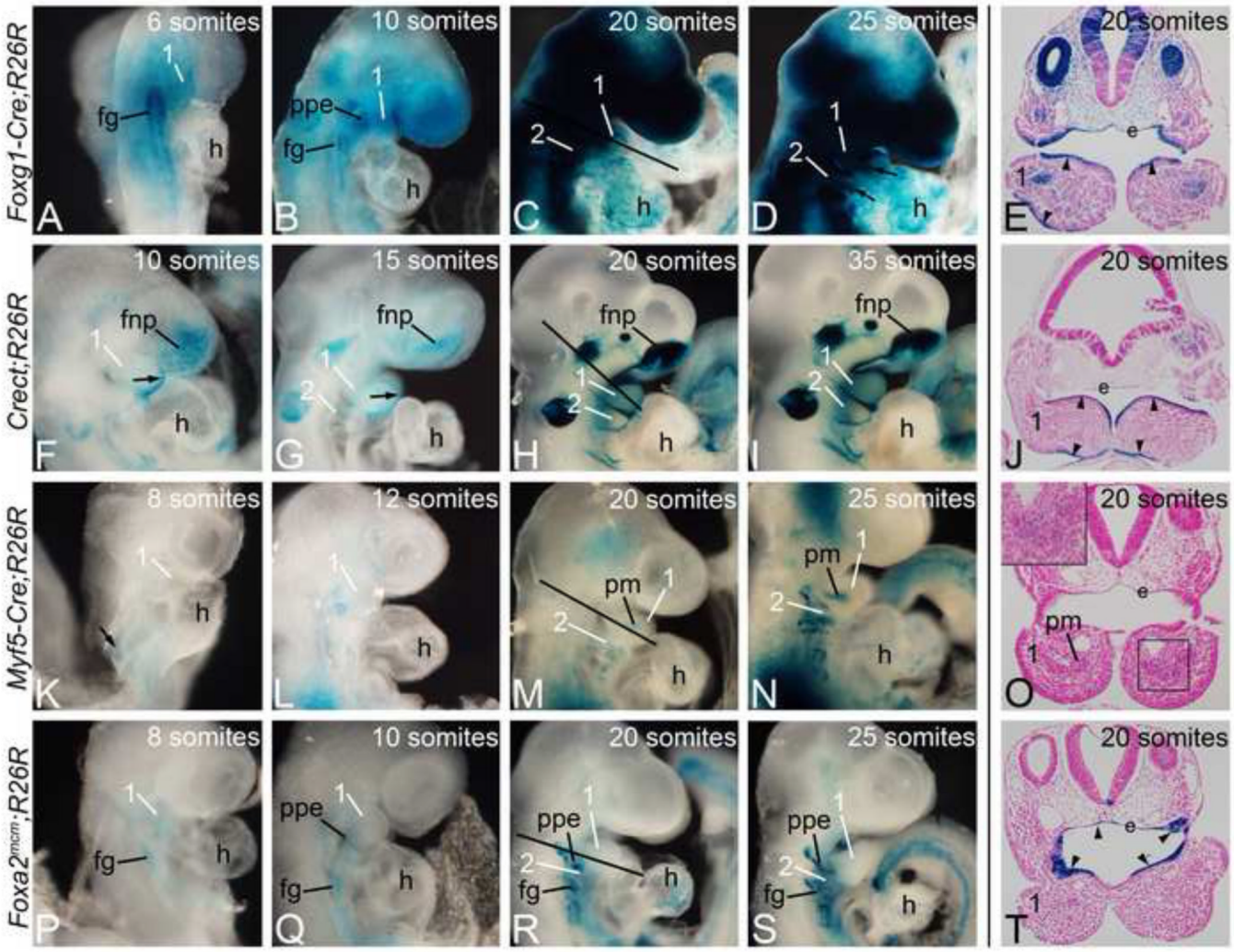

Figure 1. ***Foxg1-Cre, Crect, Myf5-Cre, and Foxa2^{mcm}*** **activity**

Cre animals were crossed into the *R26R* Cre reporter strain. Embryos were harvested between E8.0 (6 somites) and E10.5 (35 somites) and stained for β-gal activity. **A–D.** *Cre* activity in *R26R;Foxg1-Cre* embryos was found in endodermal (foregut (fg) and pharyngeal pouch endoderm (ppe)) and ectodermal structures. **E.** Transverse section through the embryo in C (20 somites) illustrates staining in the arch ectoderm (arrowheads) and endoderm (e), with staining also observed in the paraxial core mesoderm. **F–I.** β-gal activity in *R26R;Crect* embryos was found in the ectoderm of the arches (arrow) and in the frontonasal prominence (fnp). **J.** Transverse section of embryo in H showing arch ectodermal staining at 20 somites (arrowheads). **K–N.** *R26R;Myf5-Cre* embryos showed mesodermal staining that at 20 somites could be seen in the paraxial core mesoderm (pm). **O.** A transverse section through the arches in M illustrated that the staining is restricted to the core mesoderm. (inset). **P–S.** β-gal activity in *Foxa2^{mcm};R26R* embryos starts at E8.0 following tamoxifen injection at E6.5, with endodermal structures labeled (ppe, fg). **T.** Sections through the first pharyngeal pouch endoderm (e) at 20 somites shows specific β-gal activity (arrowheads). 1, mandibular pharyngeal arch; 2, second pharyngeal arch; h, heart.

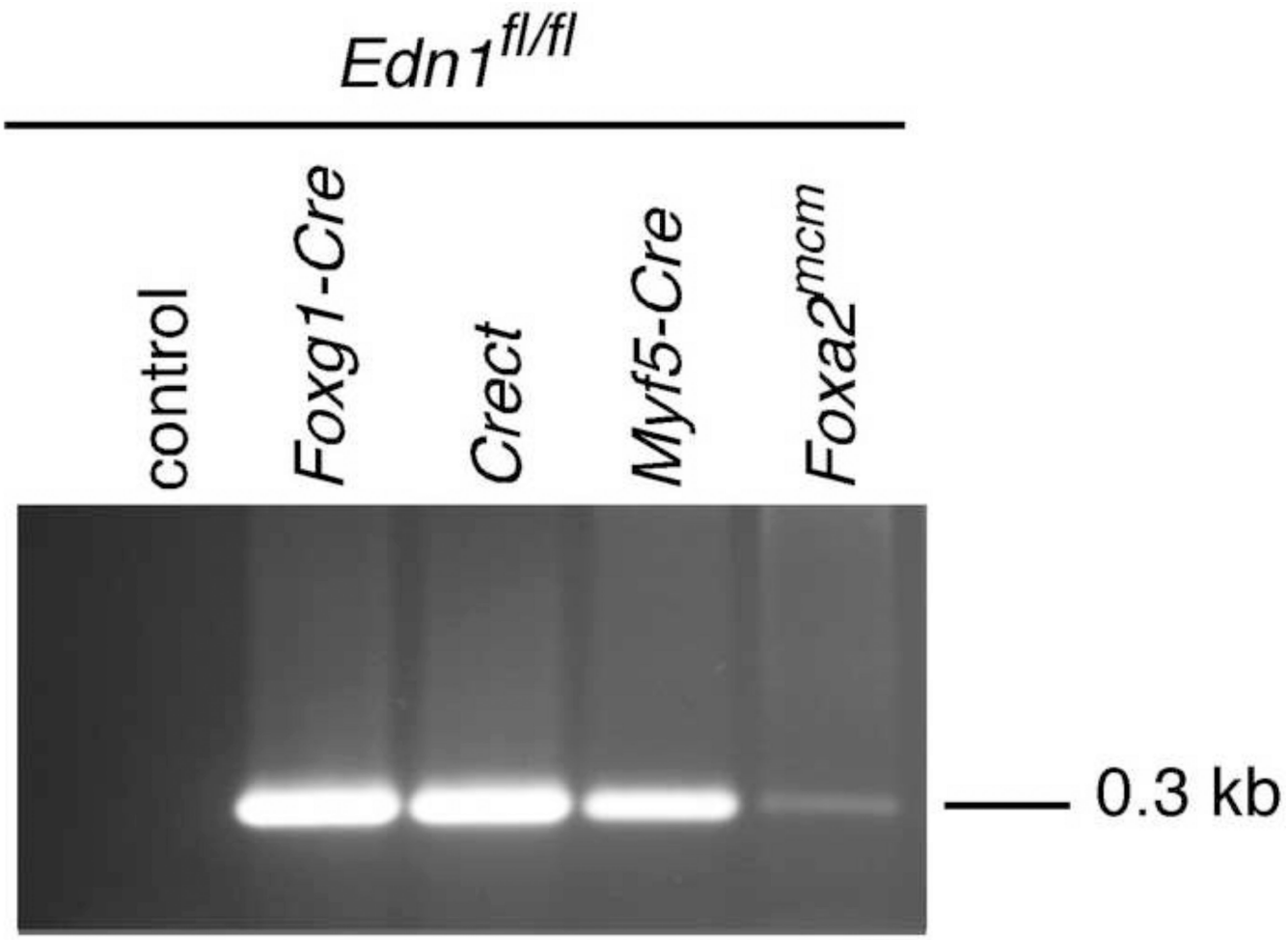

Figure 2. Analysis of Cre-mediated recombination of the *Edn1* gene in *Edn1*$^{fl/fl}$;*Cre* mice

Genomic DNA was extracted from E9.0 mouse embryo mandibular arches. Lanes 2–5 show the 300-bp band for the recombined allele. Wild-type animals show no band (lane 1).

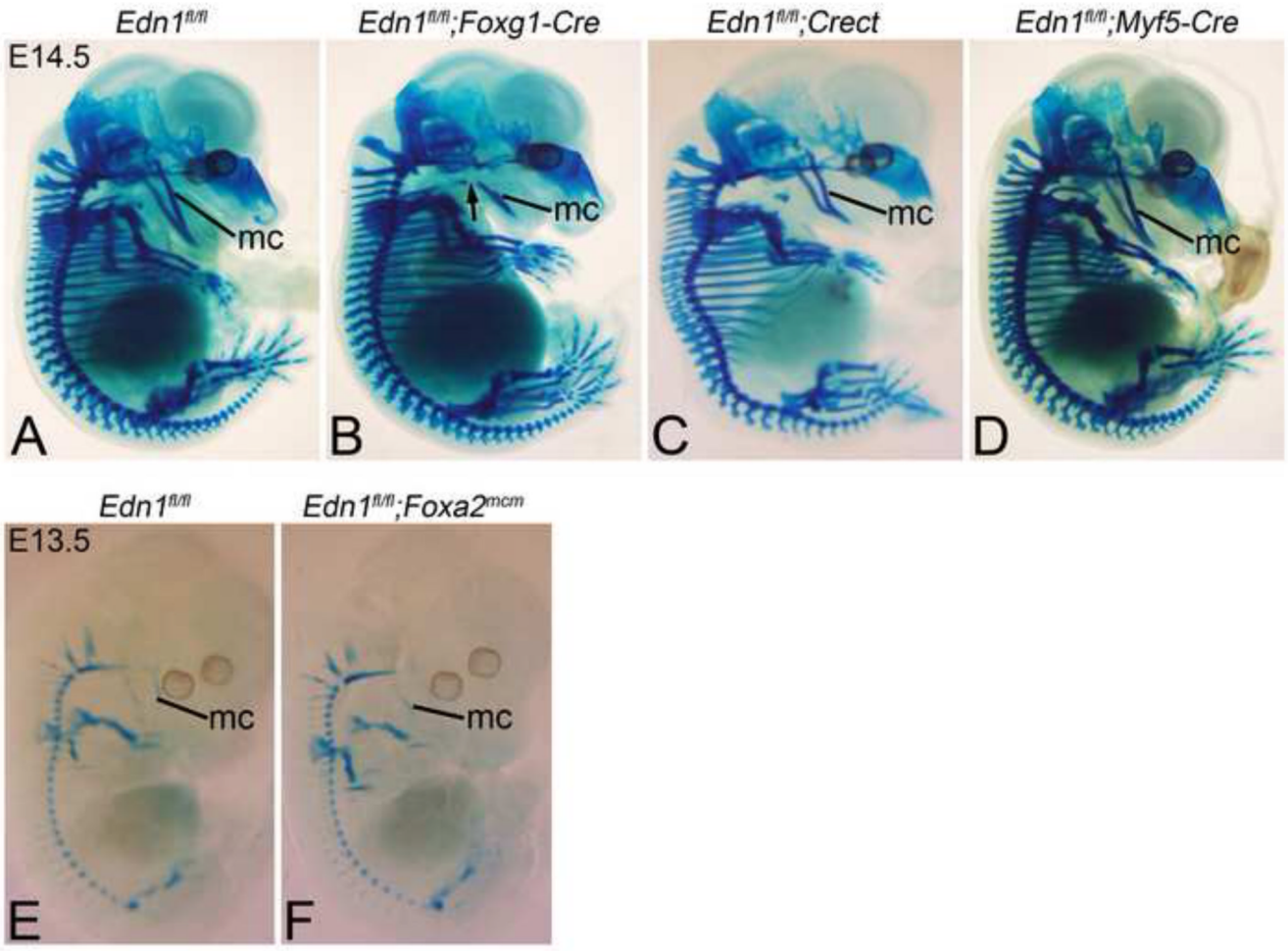

Figure 3. Analysis of early skeletal development in *Edn1* conditional mutant embryos

E14.5 (A–D) and E13.5 (E,F) control and mutant embryos stained with alcian blue to visualize cartilage. **A–D.** Lateral view displaying hypoplastic Meckel's cartilage (mc) in *Edn1*$^{fl/fl}$*;Foxg1-Cre* (B) and *Edn1*$^{fl/fl}$*;Crect* (C) embryos. Note also the interruption of Meckel's cartilage in the *Edn1*$^{fl/fl}$*;Foxg1- Cre* embryo (arrow in B) and the altered morphology in the *Edn1*$^{fl/fl}$*;Crect* embryo (arrow in C). *Edn1*$^{fl/fl}$*;Myf5-Cre* embryos (D) appear normal. **E–F.** Lateral view of *Edn1*$^{fl/fl}$ (E) and *Edn1*$^{fl/fl}$*;Foxa2*^{mcm} (F) embryos at E13.5, showing no apparent change in Meckel's cartilage morphology in the mutant.

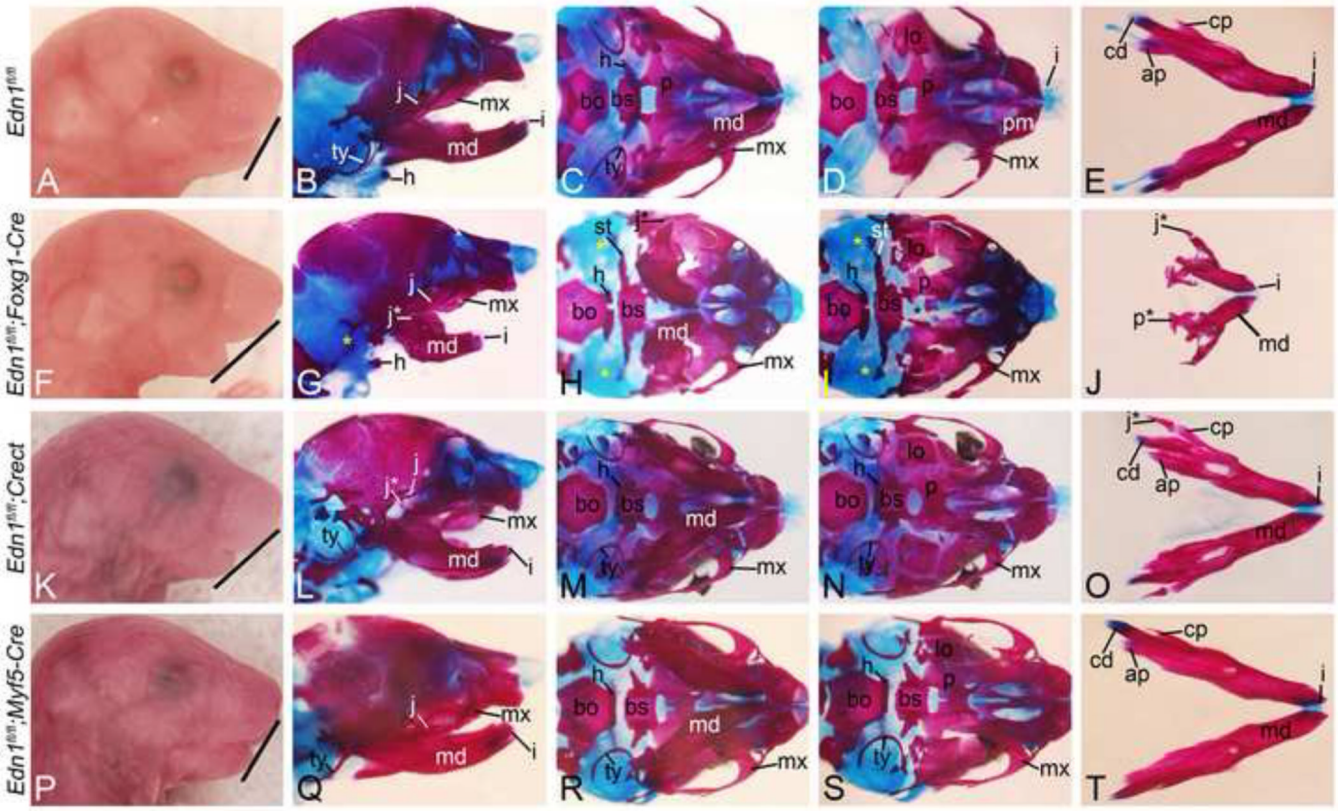

Figure 4. Characterization of cranial features in *Edn1*$^{fl/fl}$ conditional knockout embryos at E18.5

Gross morphology and alizarin red (bone) and alcian blue (cartilage)-staining of *Edn1*$^{fl/fl}$ (AE), *Edn1*$^{fl/fl}$*;Foxg1-Cre* (F–J), *Edn1*$^{fl/fl}$*;Crect* (K–O) *and Edn1*$^{fl/fl}$*;Myf5-Cre* (P–T) embryos. **B, G, L, Q.** Lateral view. **C, H, M, R.** Ventral skull view with mandible. **D, I, N, S.** Ventral view with mandible removed. **E, J, O, T.** Ventral aboral view of dissected mandibles. **A–E.** Normal craniofacial structures of an E18.5 control mouse embryo. **F–J.** *Edn1*$^{fl/fl}$*;Foxg1-Cre* embryos have a recessed lower jaw (note angle of line between A and F), deformed mandible (md) (G, H and J), absent tympanic rings (ty) (yellow * in G–I), an abnormal bone strut (st) extending from the middle ear region towards the basisphenoid (bs) (H–I), a palatal cleft (black * in I) and duplication of jugal (j*) (G, H and J) and palatine (p*) bones (J). **K–O.** *Edn1*$^{fl/fl}$*;Crect* embryos have a recessed mandible (note angle of line between A and K) and duplicated jugal bones (L and O). **P–T.** *Edn1*$^{fl/fl}$*;Myf5-Cre* embryo craniofacial structures are normal. ap, angular process; bo, basisoccipital; cd, condyloid process; cp, coronoid process; h, hyoid; i, incisors; j, jugal; lo, lamina obturans; mx, maxilla; p, palatine.

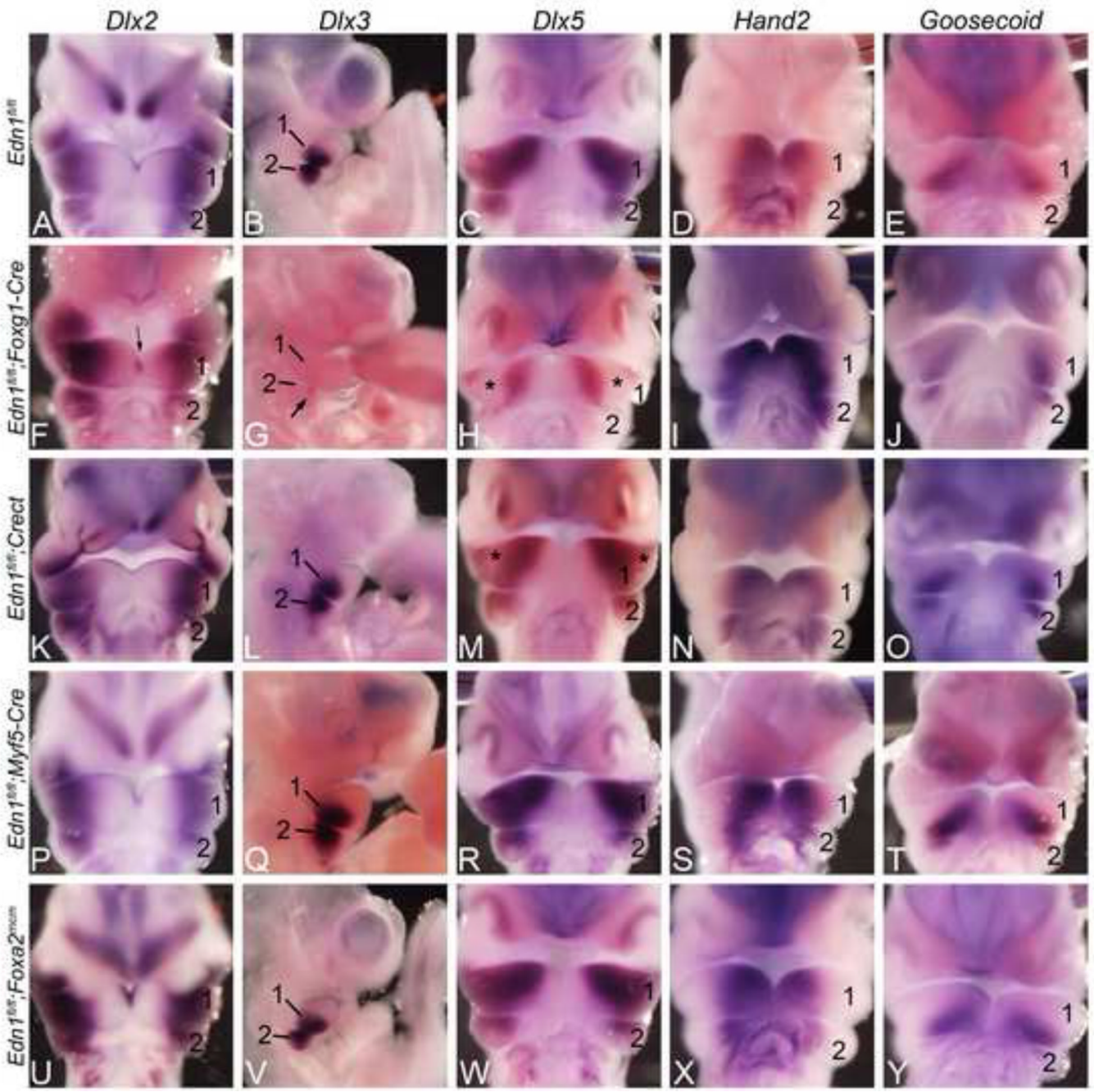

Figure 5. Whole-mount in situ hybridization (ISH) analysis in E10.5 *Edn1*$^{fl/fl}$ conditional knockout embryos

Ventral view of embryos after ISH for *Dlx2* (A, F, K, P, U), *Dlx5* (C, H, M, R, W), *Hand2* (D, I, N, S, X) and *Goosecoid* (E, J, O, T, Y). The heart has been removed to aid in visualization. B, G, L, Q, V show a lateral view of embryos after ISH for *Dlx3*. **A–E.** Expression in E10.5 control embryos. **F–J.** In *Edn1*$^{fl/fl}$*;Foxg1-Cre* embryos, *Dlx2* expression was disrupted in the distal ectoderm of the mandibular first pharyngeal arch (arrows in F). *Dlx3* expression was almost completely lost in the first pharyngeal arch and reduced in the second pharyngeal arch (arrow in G). *Dlx5* expression was disrupted, but only in a band across the central mandibular arch (asterisks in H). *Hand2* (I) and *Goosecoid* (J) expression

appeared unaffected. **K–O.** *Dlx5* expression in *Edn1*$^{fl/fl}$*;Crect* embryos was also disrupted (asterisks in M).Expression of other genes examined was unaffected. **P–Y.** The expression of all five genes was unaffected in *Edn1*$^{fl/fl}$*;Myf5-Cre* (P–T) and *Edn1*$^{fl/fl}$*;Foxa2*^{mcm} (U–Y) embryos. 1, mandibular pharyngeal arch; 2, second pharyngeal arch.

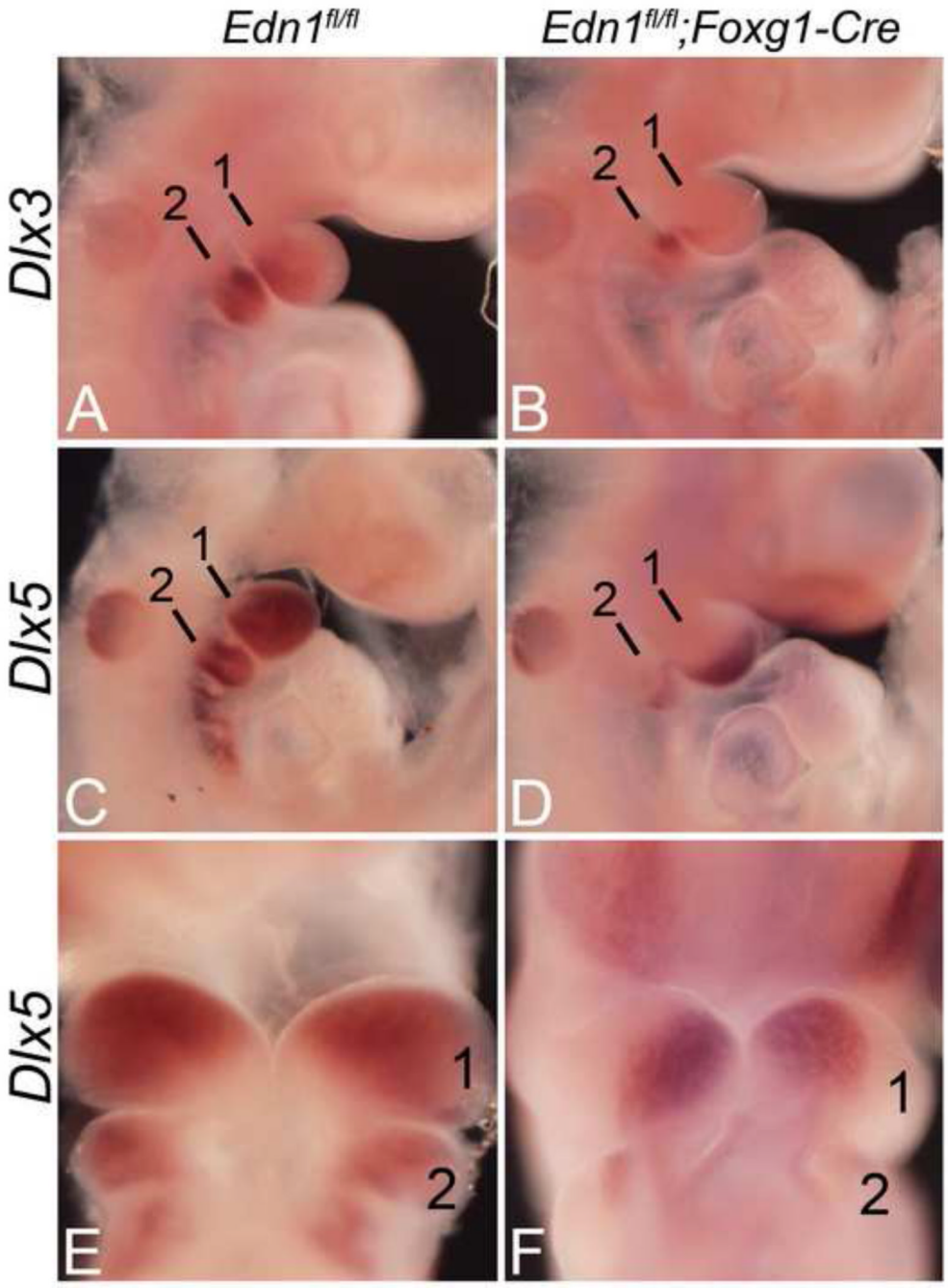

Figure 6. Whole-mount in situ hybridization (ISH) analysis in E9.5 *Edn1$^{fl/fl}$;Foxg1-Cre* embryos

Lateral (A–D) and ventral (E–F) views of embryos after ISH for *Dlx3* and *Dlx5*. **A–B.** *Dlx3* expression was almost completely absent in the first arch of E9.5 *Edn1$^{fl/fl}$;Foxg1-Cre* embryos (B). **C–F.** Although *Dlx5* expression was present in *Edn1$^{fl/fl}$;Foxg1-Cre* embryos, expression was confined to the distal half of the mandibular arch (D, F). 1, mandibular pharyngeal arch; 2, second pharyngeal arch

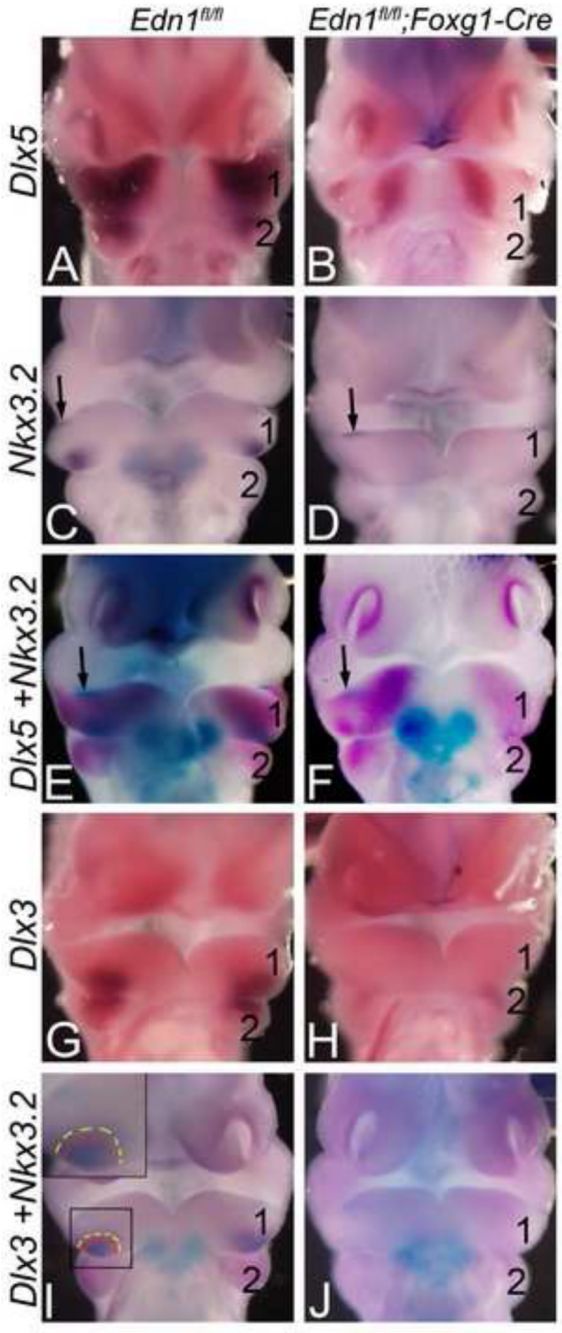

Figure 7. The *Nkx3.2* and *Dlx5* expression domains overlap in the mandibular arch and demarcate the intermediate domain

Ventral view of E10.5 *Edn1*$^{fl/fl}$*;Foxg1-Cre* embryos after single (A–D; G–H) or double (E–F; I–J) ISH for *Dlx3, Dlx5* and *Nkx3.2*. **A–B.** *Dlx5* expression is disrupted in a strip of the mandibular arch mesenchyme of mutant embryos (B). **C–D.** Expression of the intermediate domain marker *Nkx3.2* is also disrupted in the mandibular arch mesenchyme of mutant embryos (D). **E–F.** Double ISH for *Dlx5* (magenta) and *Nkx3.2* (blue) shows that in the mutant embryos, the residual *Nkx3.2* mesenchyme expression (arrow in F) is confined to the domain in which *Dlx5* is absent. **G–H.** *Dlx3* expression is absent in the mandibular arch mesenchyme of mutant embryos. **I–J.** Double ISH for *Dlx3* and *Nkx3.2* shows that *Nkx3.2*

mesenchyme expression (blue) is contained within the *Dlx3* mesenchyme domain (magenta) in control embryos (I). This overlapping expression is absent in E10.5 *Edn1*$^{fl/fl}$*;Foxg1-Cre* embryos (J). 1, mandibular pharyngeal arch; 2, second pharyngeal arch.

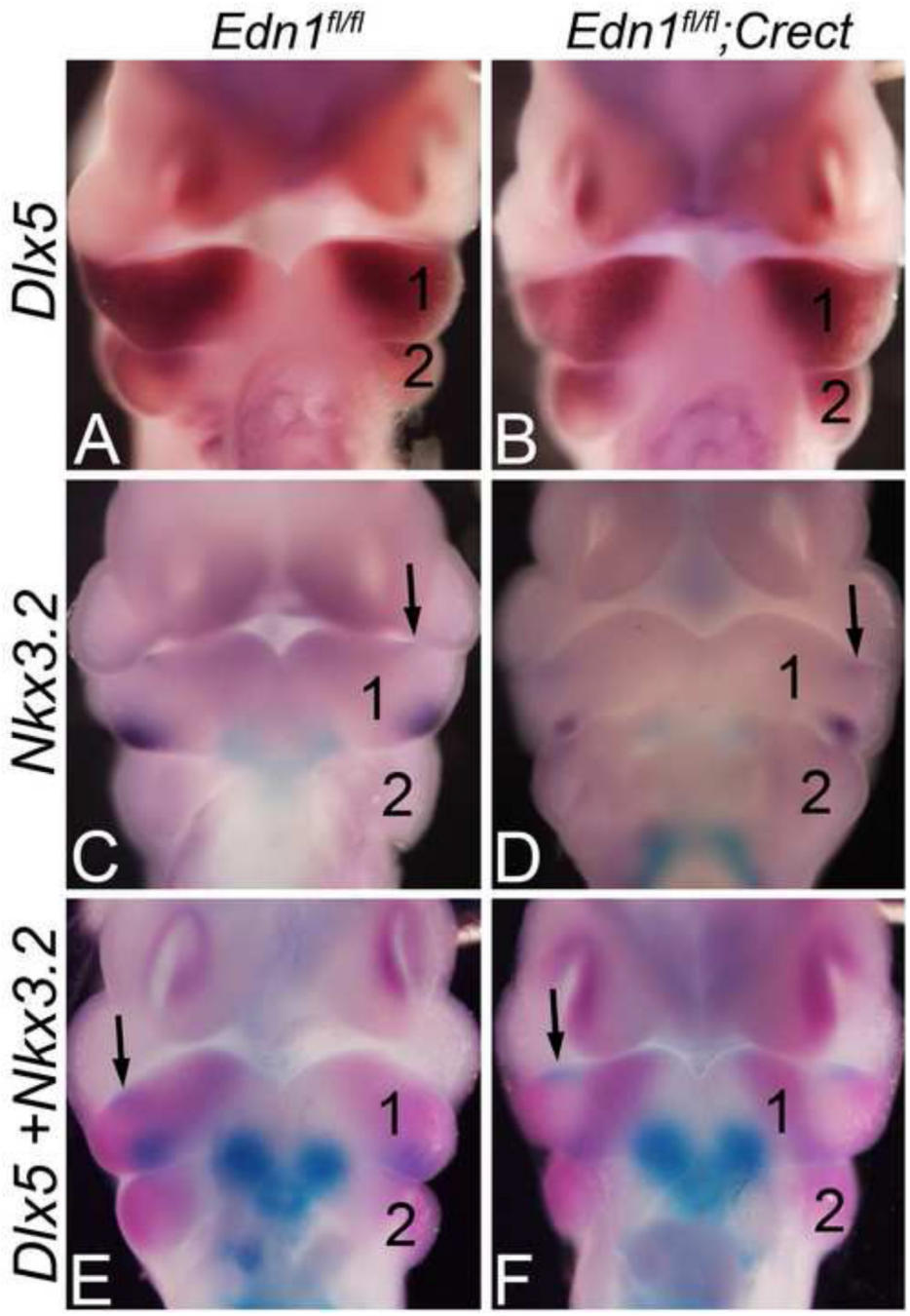

Figure 8. ***Nkx3.2*** **expression is disrupted in the intermediate mandibular arch domain of** ***Edn1*** $^{fl/fl}$ ***;Crect*** **embryos**

Ventral view of E10.5 *Edn1* $^{fl/fl}$ *;Crect* embryos after single (A–D) or double (E–F) ISH for *Dlx5* and/or *Nkx3.2*. **A–B.** *Dlx5* expression is disrupted in a strip of the mandibular arch mesenchyme in *Edn1* $^{fl/fl}$ *;Crect* embryos (B). **C–D.** Mesenchymal expression of *Nkx3.2* is disrupted in the mandibular of *Edn1* $^{fl/fl}$ *;Crect* embryos, while epithelial expression (arrow) is unaffected (D). **E–F.** Double ISH for *Dlx5* (magenta) and *Nkx3.2* (blue) expression. In control embryos, mesenchymal expression of both genes overlaps (E). In *Edn1* $^{fl/fl}$ *;Crect* embryos, mesenchymal *Nkx3.2* expression is largely absent from the domain in which *Dlx5* expression has been lost (F). 1, mandibular pharyngeal arch; 2, second pharyngeal arch.